

GUIDED-SPATIO-TEMPORAL FILTERING FOR EXTRACTING SOUND FROM OPTICALLY MEASURED IMAGES CONTAINING OCCLUDING OBJECTS

Risako Tanigawa, Kohei Yatabe, Yasuhiro Oikawa

Department of Intermedia Art and Science, Waseda University, Tokyo, Japan

ABSTRACT

Recent development of optical interferometry enables us to measure sound without placing any device inside the sound field. In particular, parallel phase-shifting interferometry (PPSI) has realized advanced measurement of refractive index of air. Its novel application investigated very recently is simultaneous visualization of flow and sound, which had been difficult until PPSI enabled high-speed and accurate measurement several years ago. However, for understanding aerodynamic sound, separation of air flow and sound is necessary since they are mixed up in the observed video. In this paper, guided-spatio-temporal filtering is proposed to separate sound from the optically measured images. Guided filtering is combined with a physical-model-based spatio-temporal filterbank for extracting sound-related information without the undesired effect caused by the image boundary or occluding objects. Such image boundary and occluding objects are typical difficulty arose in signal processing of an optically measured sound filed.

Index Terms— Guided filter, spatio-temporal filterbank, optical visualization, high-speed imaging, aerodynamic sound.

1. INTRODUCTION

Flow-induced sound, which is often called aerodynamic sound, is one of the causes of the noise of high-speed trains and automobiles [1, 2]. In accordance with the increase of their speed, demand for reduction of aerodynamic noises has been increasing. However, measuring aerodynamic sound is not easy because microphones cannot be installed inside the flow. Placing microphones inside the flow disturbs the flow field, which results in another cause of flow-induced sound, and wind noise is also problematic for sound measurement [3, 4].

Recent development of optical interferometry enables us to measure sound without placing any device inside the sound field. In particular, parallel phase-shifting interferometry (PPSI) has realized instantaneous measurement of sound pressure as images with accuracy applicable for audible range [5–11]. This very recent method allows us to simultaneously measure flow and sound [12–15] (see Fig. 8 for an example), which had been difficult until PPSI has combined with a high-speed polarization camera [5]. That is, PPSI has opened up a new way of investigating flow-induced sound.

However, for detailed investigation of flow-induced sound, separation of flow and sound is necessary. Since PPSI measures flow and sound through the refractive index of air, both phenomena are mixed up in the measured images. Therefore, they should be separated before interpreting the images. For extracting sound from observed mixture, linear filtering has been applied in optical sound measurement [16–18]. Especially, the physical-model-based spatio-temporal filter has been successfully applied to extract information only related to sound [16, 17]. The filter aims to pass components satisfying the wave equation and stop other components. Although this

property should be desirable for the flow-sound separation, the performance of filtering is degraded around the image boundary since any information outside the image is not contained in the data. Moreover, optically measured sound fields often contain occluding objects which shade the measuring light of the laser and create unmeasured regions inside the images. That is, uniform filtering fails around the image boundary which also exists inside the image of optical sound measurement containing occluding objects.

In this paper, a translation-variant filter, namely guided filter, is combined with the physical-model-based spatio-temporal filter for extracting sound from optically measured images. A guided filter is an image filter based on a local linear model [19, 20] which is edge-preserving as the bilateral filter [21] with lower computational cost. Its filter kernel (or impulse response) varies at each position, where the rule for variation depends on the user-defined guidance image. We propose to use the guided filter for spatial filtering in the spatio-temporal filter with a mask as the guidance which informs the position of the image boundary and occluding objects. Through some experiments using both simulated and measured sound fields, it is confirmed that the proposed method can filter the data without the effect of the occluding objects.

2. OPTICAL MEASUREMENT OF SOUND FIELD

Optical measurement of sound has gained much attention in recent years as an alternative to a microphone [22–24]. It utilizes the nature of the phase of light modulated by the refractive index of a medium:

$$\phi(\mathbf{r}, t) = k \int_L n(\mathbf{l}, t) d\mathbf{l}, \quad (1)$$

where ϕ is the phase of light, \mathbf{r} is the position vector, t is the time, k is the wave number of light, L is the optical path, and n is the refractive index of the medium. Since the refractive index of air $n(\mathbf{r}, t)$ is related to the sound pressure $p(\mathbf{r}, t)$ as

$$n(\mathbf{r}, t) = n_0 + \frac{n_0 - 1}{\gamma p_0} p(\mathbf{r}, t), \quad (2)$$

where p_0 is the atmospheric pressure, n_0 is its refractive index, and γ is the specific heat ratio of the air [25], substituting this equation into Eq. (1) indicates that the sound pressure $p(\mathbf{r}, t)$ can be measured through the phase of light $\phi(\mathbf{r}, t)$.

However, directly measuring the phase of light is difficult since the frequency of light is extremely high. Therefore, interference of light has been widely used as a method of observing the phase of light. After converting the phase into light intensity through interference, an estimation technique of the phase from intensity, which is usually called phase retrieval, is required. The phase-sifting interferometry (PSI) [26] is one of the most widely used methods for accurately retrieving the phase using multiple interference fringes.

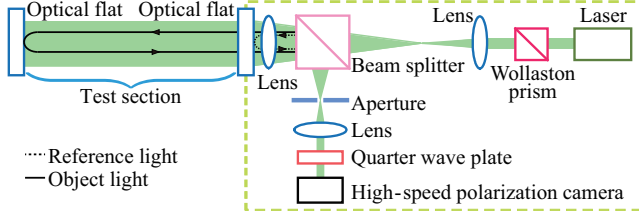


Fig. 1. Schematic of the PPSI system used in our research.

While PSI has been successfully applied to measurement of static objects, it had been difficult to apply PSI to time-varying phenomena because multiple measurements are necessary for phase retrieval.

PPSI is a parallelized version of PSI so that multiple interference fringes can be acquired simultaneously [27, 28]. While usual PSI requires change of the optical setting for each measurement, which limits its use to time-invariant phenomena, PPSI as in Fig. 1 handles interference in polarization state of the light. Then, multiple interference fringes can be obtained by a polarization camera whose high-speed version has very recently realized [29]. Hence, it enables us to measure a time-varying sound field up to 750 kHz, in theory.

2.1. Physical-model-based spatio-temporal filtering [17]

Although it is possible to optically observe a time-varying sound field, the quality of observation depends on the magnitude of the sound pressure. Since typical audible sound requires measurement of 0.1 nm variation in terms of optical path length [5], the observed sound field is often contaminated by severe noise. For removing the noise and extracting sound, the spatio-temporal filtering was proposed based on the physical model of sound, or the wave equation [16, 17]. By considering the homogeneous wave equation in the frequency domain, the homogeneous Helmholtz equation,

$$(\Delta + k^2) p(\mathbf{r}, \omega) = 0, \quad (3)$$

is obtained, where ω is the angular frequency, $k = \omega/c$ is the wave number (c is the speed of sound), and Δ is the Laplace operator. It is well-known that the solution to the Helmholtz equation can be approximated arbitrarily well by the plane wave,

$$p(\mathbf{r}, \omega) \simeq \sum_n \alpha_n \psi_n(\mathbf{r}, \omega), \quad (4)$$

where α_n is the n th coefficient, and ψ_n is the plane wave propagating to n th direction whose wave number is k . As the spatial spectrum of a plane wave is the delta function on the circle whose radius is $k = \omega/c$, the spatio-temporal spectrum of a function satisfying the wave equation is concentrated on the collection of such circles.

Based on this concentration of the spatio-temporal spectrum of sound components, the spatio-temporal filterbank was proposed to pass the spectrum related to sound and stop other parts [17]. As illustrated in Fig. 2, after applying temporal analysis filterbank, spatial filters whose cutoff frequencies are decided by the above physical model are applied. Although it has been shown to be effective, its performance is degraded around the image boundary because such artificial boundary (defined by the viewing angle of the camera) is not considered in the above model. The occluding objects, which often arise in the optical sound measurement, is also problematic because the boundary condition cannot be considered properly for such objects. To circumvent such performance degradation caused by the spatial filters, which have been designed based on the above linear model, they must be modified around the boundaries.

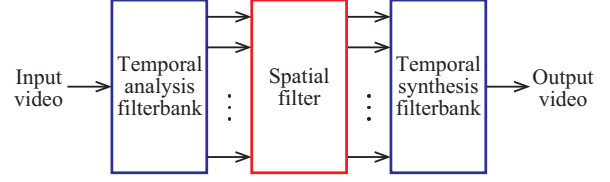


Fig. 2. Flow chart of the spatio-temporal filterbank.

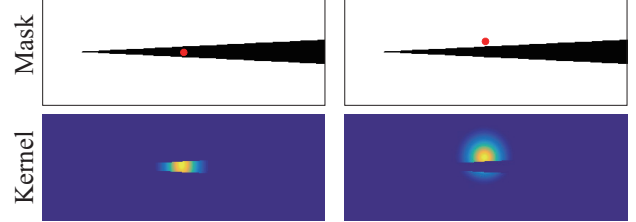


Fig. 3. Filter kernel (impulse response) of the guided filter at different positions. Red points indicate the positions for the filter kernel. The wedge-shaped edge is an object which appears in our experiment (see Fig. 7). The image size was 150×400 pixels.

3. PROPOSED METHOD

To circumvent the performance degradation occurring around the image boundary and occluding objects, we propose to integrate a guided filter [19, 20] into the spatio-temporal filterbank.

A guided filter is a translation-variant filter whose filter kernel (or impulse response) varies at each position according to the guidance image. Let the input and output image be denoted by I_{in} and I_{out} . Then, a guided filter considers the following local linear model:

$$I_{out}(n) = a_m G(n) + b_m \quad (\forall n \in \mathcal{W}_m), \quad (5)$$

where G is the guidance image, n is the index of the image pixel¹, \mathcal{W}_m is the m th region of a sliding window (region corresponding to the filter kernel centered at m th pixel), and a_m and b_m are some coefficients for the m th region. These coefficients are determined for each m by the regularized least squares method as

$$\arg \min_{a_m, b_m} \sum_{n \in \mathcal{W}_m} (a_m G(n) + b_m - I_{in}(n))^2 + \lambda a_m^2, \quad (6)$$

where $\lambda > 0$ is a regularization parameter. Its solution is given by

$$a_m = \text{cov}_m[G, I_{in}] / (\text{var}_m[G] + \lambda), \quad (7)$$

$$b_m = \text{mean}_m[I_{in}] - a_m \text{mean}_m[G], \quad (8)$$

where $\text{mean}_m[\cdot]$, $\text{var}_m[\cdot]$ and $\text{cov}_m[\cdot, \cdot]$ are the mean, variance and covariance within \mathcal{W}_m , respectively. Since these coefficients vary depending on \mathcal{W}_m , and $I_{in}(n)$ is contained in multiple \mathcal{W}_m , the output image is obtained by the average of them:

$$I_{out}(n) = \text{mean}_n[a] G(n) + \text{mean}_n[b]. \quad (9)$$

Although this filter is translation-variant, it can be efficiently applied to image sequences because, after storing $\text{mean}_m[G]$ and $\text{var}_m[G]$ (calculating by linear filtering), only four linear filtering are required. The nature of the filter is fully controlled by the guidance image G , and therefore choosing it appropriately is important, which depends on the application.

¹Although an image has two dimensions corresponding to the horizontal and vertical axes usually indexed by two integers, the whole pixels are indexed by a single integer n here as in the original paper [19].

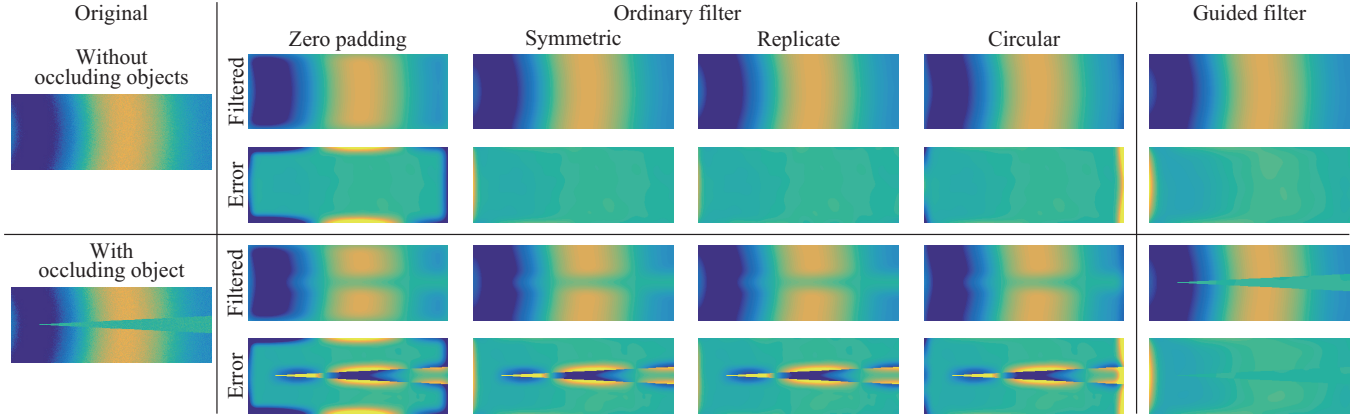


Fig. 4. Filtered results of the simulated data (SNR: 20 dB). The error is shown with the same amount of magnification for better visibility.

3.1. Proposed guided-spatio-temporal filterbank

For integrating a guided filter into the spatio-temporal filterbank, we propose two concepts related to the guided filtering: (i) deciding the filter response by the physical model of sound in Section 2.1, and (ii) choosing the guidance image G as a mask of occluding objects.

For considering the cutoff frequency of the spatial filters as described in Section 2.1, filter kernel of the guided filter must be modified. To do so, we consider the weighted least squares method:

$$\arg \min_{a_m, b_m} \sum_{n \in \mathcal{W}_m} w_{n,m} ((a_m G(n) + b_m - I_{in}(n))^2 + \lambda a_m^2), \quad (10)$$

where $w_{n,m} \geq 0$ is the weight deciding the frequency response. This change of the formulation can be easily managed by modifying $\text{mean}_m[\cdot]$, $\text{var}_m[\cdot]$ and $\text{cov}_m[\cdot, \cdot]$ in Eqs. (7) and (8) to their weighted versions [19, 20]. We construct this weight from the physical model as in the original spatio-temporal filtering in [17] because it corresponds to the filter kernel (impulse response) in the usual translation-invariant filtering.

While it is straightforward to choose the weight according to [17], choice of the guidance image needs care because it deforms the filter kernel at each position. Since we want to circumvent the effect of occluding objects, a guidance image should be constructed based on the position of them. To minimize the effect of the guidance onto the frequency response, we propose to use a binary mask of the occluding objects which is common in the optical interferometry, especially for phase unwrapping [30, 31]. An example of the mask image together with the corresponding filter kernel (impulse response) is shown in Fig. 3. The mask image consists of 0 (black) and 255 (white) as usual in image processing. The red circles in upper represent the center positions of \mathcal{W}_m , and the bottom row shows the corresponding kernel. This figure clearly illustrates that the guided filter with the mask as the guidance independently process the regions inside and outside the occluding object. Therefore, information related to sound can be extracted as explained in Section 2.1 without the fear of existence of the occluding objects. Note that the magnitude of the filter kernel is automatically normalized within the process of guided filtering in Eqs. (7)–(9) owing to the statistical operations.

The proposed guided-spatio-temporal filterbank is realized by replacing the spatial filters with the mask-guided filter whose weight is constructed as in the original version. As shown in the next section, the proposed method can avoid the undesired artifacts of the spatial filtering caused by existence of the occluding objects.

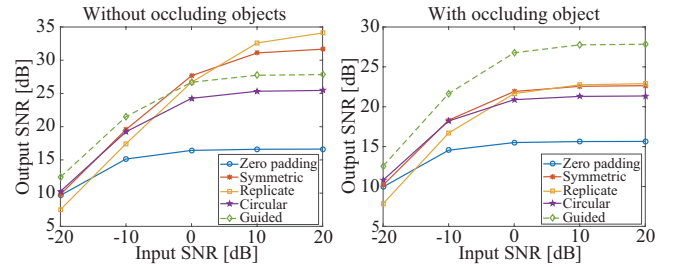


Fig. 5. SNR of filtered images when SNR of the input image was varied from -20 to 20 dB at intervals of 10 dB.

4. EXPERIMENTS

We conducted two experiments, numerical simulation and measurement, for confirming the effectiveness of the proposed method.

4.1. Application to simulated sound filed

Firstly, denoising performance is investigated through simulated data. Simulated noisy sound fields, with and without occluding objects, were spatially filtered by the proposed guided filter. A wedge-shaped edge, which is frequently considered in the area of aeroacoustics as it produces the well-studied “edge tone” [32, 33], was simulated for the occluding object to relate the simulation result with the measurement experiment in the next subsection. For comparison, the linear translation-invariant version of the filter with four boundary conditions were also applied to the same data. The boundary conditions of the usual version were (i) zero padding outside the image region, (ii) copying symmetrically reflected image with respect to the boundary, (iii) padding replication of the image values at the boundary, and (iv) copying circularly and periodically shifted image. The signal-to-noise ratios (SNRs) of the input images varied from -20 to 20 dB at the intervals of 10 dB by adding the Gaussian noise.

The results of filtering are shown in Fig. 4, where the SNR of the input image was 20 dB. All the results except the zero padding condition seem to have a similar error when the occluding object did not exist inside the image. On the other hand, the error increased notably for the ordinary filtering when the occluding object existed. Only the proposed mask-guided filter obtained the result with a small error which seems quite similar to that without the object. That is,

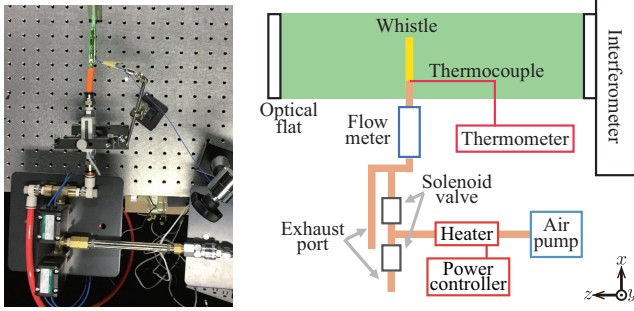


Fig. 6. Experimental setup for the measurement of the sound and flow radiated from a whistle.

the mask-guided filter can ignore the occluding object and correctly extract the sound field around it.

For quantitative evaluation, SNR of the filtered images of Fig. 4 are summarized in Fig. 5. For fair comparison, SNR of the filtered result was calculated without including the region of the occluding object because the error inside that region can be removed when the mask is available as for the proposed mask-guided filter. Comparing the figures on left and right, SNR of usual filtering with the occluding object was reduced by 5 to 10 dB compared to those without occluding objects. In contrast, SNR of the mask-guided filtering with the occluding object was almost the same as that without the occluding object, which resulted in higher SNR than the others when the object existed inside the image. These results suggested that the proposed mask-guided filter can be safely applied to the optically measured sound field without fear of the occluding objects.

4.2. Application to data measured by PPSI

As a real application, the proposed method was applied to three types of measured data for confirming extraction of sound from optically measured images including the air flow and occluding objects. The three data measured by the PPSI system are the following: (i) a sound field radiated from a loudspeaker with air flow blown from a hose as a test data of visualization containing both sound and flow (speaker+hose), (ii) sound and air flow radiated from a whistle (whistle), and (iii) sound generated by the edge tone phenomena caused by air flow (edge tone). These data cannot be captured by any other measurement method but PPSI. The experimental setup for each of these measurements are detailed in the following:

speaker+hose The loudspeaker was installed at the bottom of the imaging area where the tip of the loudspeaker is slightly apparent inside the imaging area. The air flow was blown from the upper-left corner of the imaging area. The driving signal of the loudspeaker was 8 kHz sinusoidal signal.

whistle The setup of the whistle is shown in Fig. 6 [13]. The whistle emitting sound around 12 kHz was installed at the bottom of the imaging area. The air flow blown into the whistle was heated by the heater for visualizing the incompressible flow.

edge tone The setup of the edge tone is shown in Fig. 7 [14], where the left figure shows the edge tone generator consisted of the nozzle and the wedge-shaped edge, and the right figure shows schematic of the experimental setup. The nozzle outlet was 1 mm in height and 25 mm in width, while the angle of the edge was 20 degrees and the width was 50 mm. The heated air was blown into the nozzle, and the generated sound by the edge tone phenomena was about 1.2 kHz.

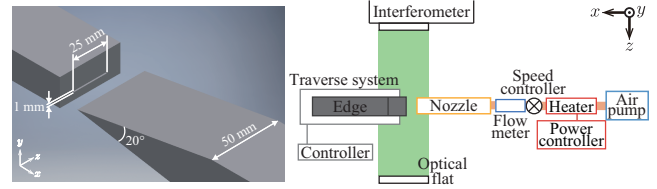


Fig. 7. Experimental setup for the measurement of the edge tone.

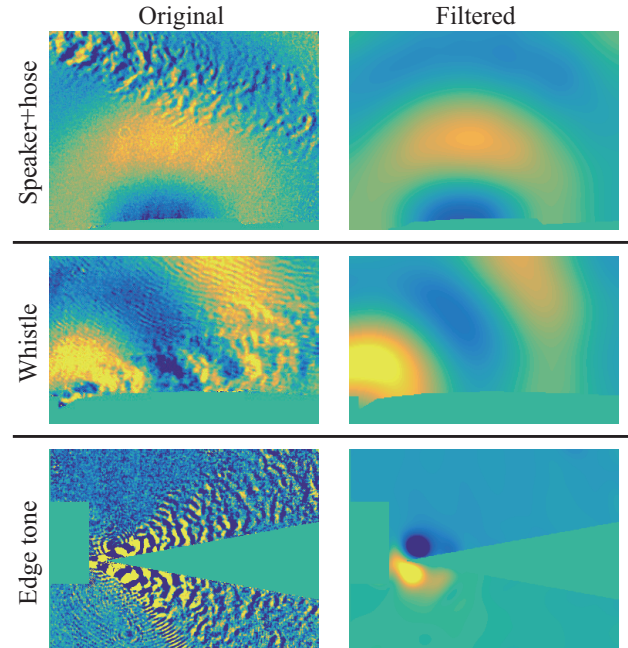


Fig. 8. Measured data and the corresponding filtered result by the proposed guided-spatio-temporal filterbank.

The results of the filtered images are shown in Fig. 8, where the measurement noise was greatly reduced by both temporal and spatial filtering. The sound fields were extracted from the data including air flow even near the occluding objects. These results suggest that the proposed guided-spatio-temporal filtering is effective for extracting the sound field measured by PPSI. Note that, in the edge tone, the sound cannot be observed until the filter was applied to remove the air flow because the sound pressure level was not satisfactory for PPSI. Therefore, the proposed method is essential for observing such small sound around an occluding object and/or with physical phenomena not related to sound such as air flow.

5. CONCLUSION

In this paper, guided-spatio-temporal filtering was proposed for extracting sound from optically measured data including occluding objects. By utilizing the mask image as the guidance of the guided filter, the undesired effect of the occluding object can be circumvented through the translation-variant nature of filter kernel. The proposed method was tested with the actual aerodynamic sound, and its effectiveness was confirmed. Since the proposed method is essential to some situation when the sound is small for optical measurement, it would be helpful for understanding the nature of the generation of aerodynamic sound. Future works include application of the proposed method for such physical investigation.

6. REFERENCES

- [1] C. Mellet, F. Létourneaux, F. Poisson, and C. Talotte, "High speed train noise emission: Latest investigation of the aerodynamic/rolling noise contribution," *J. Sound Vib.*, vol. 293, no. 3, pp. 535–546, 2006.
- [2] P. J. Morris and G. M. Lilley, *Aerodynamic Noise: Theory and Applications*, chapter 9, pp. 128–158, Wiley-Blackwell, 2008.
- [3] G. P. van den Berg, "Wind-induced noise in a screened microphone," *J. Acoust. Soc. Am.*, vol. 119, no. 2, pp. 824–833, 2006.
- [4] J. A. Zakis and C. M. Tan, "Robust wind noise detection," in *2014 IEEE Int. Conf. Acoust. Speech Signal Process. (ICASSP)*, May 2014, pp. 3655–3659.
- [5] K. Ishikawa, K. Yatabe, N. Chitanont, Y. Ikeda, Y. Oikawa, T. Onuma, H. Niwa, and M. Yoshii, "High-speed imaging of sound using parallel phase-shifting interferometry," *Opt. Express*, vol. 24, no. 12, pp. 12922–12932, Jun 2016.
- [6] K. Ishikawa, K. Yatabe, Y. Ikeda, Y. Oikawa, T. Onuma, H. Niwa, and M. Yoshii, "Optical sensing of sound fields: non-contact, quantitative, and single-shot imaging of sound using high-speed polarization camera," *Proc. Meet. Acoust. (POMA)*, vol. 29, no. 1, pp. 030005, 2016.
- [7] K. Ishikawa, K. Yatabe, Y. Ikeda, Y. Oikawa, T. Onuma, H. Niwa, and M. Yoshii, "Interferometric imaging of acoustical phenomena using high-speed polarization camera and 4-step parallel phase-shifting technique," *Proc. SPIE*, vol. 10328, pp. 10328–10328–7, 2017.
- [8] Y. Oikawa, K. Ishikawa, K. Yatabe, T. Onuma, and H. Niwa, "Seeing the sound we hear: optical technologies for visualizing sound wave," *Proc. SPIE*, vol. 10666, pp. 10666–10666–8, 2018.
- [9] K. Yatabe, K. Ishikawa, and Y. Oikawa, "Improving principal component analysis based phase extraction method for phase-shifting interferometry by integrating spatial information," *Opt. Express*, vol. 24, no. 20, pp. 22881–22891, Oct 2016.
- [10] K. Yatabe, K. Ishikawa, and Y. Oikawa, "Simple, flexible, and accurate phase retrieval method for generalized phase-shifting interferometry," *J. Opt. Soc. Am. A*, vol. 34, no. 1, pp. 87–96, Jan 2017.
- [11] K. Yatabe, K. Ishikawa, and Y. Oikawa, "Hyper ellipse fitting in subspace method for phase-shifting interferometry: practical implementation with automatic pixel selection," *Opt. Express*, vol. 25, no. 23, pp. 29401–29416, Nov 2017.
- [12] K. Ishikawa, R. Tanigawa, K. Yatabe, Y. Oikawa, T. Onuma, and H. Niwa, "Simultaneous imaging of flow and sound using high-speed parallel phase-shifting interferometry," *Opt. Lett.*, vol. 43, no. 5, pp. 991–994, Mar 2018.
- [13] R. Tanigawa, K. Ishikawa, K. Yatabe, Y. Oikawa, T. Onuma, and H. Niwa, "Optical visualization of a fluid flow via the temperature controlling method," *Opt. Lett.*, vol. 43, no. 14, pp. 3273–3276, Jul 2018.
- [14] R. Tanigawa, K. Ishikawa, K. Yatabe, Y. Oikawa, T. Onuma, and H. Niwa, "Optical visualization of sound source of edge tone using parallel phase-shifting interferometry," in *47th Int. Congr. Expo. Noise Control Eng. (Inter-Noise 2018)*, Aug 2018.
- [15] R. Tanigawa, K. Yatabe, and Y. Oikawa, "Interferometric measurement of aerodynamic sound generated by parallel plates inside flow field," in *48th Int. Congr. Expo. Noise Control Eng. (Inter-Noise 2019)*, June 2019.
- [16] N. Chitanont, K. Yaginuma, K. Yatabe, and Y. Oikawa, "Visualization of sound field by means of schlieren method with spatio-temporal filtering," in *2015 IEEE Int. Conf. Acoust. Speech Signal Process. (ICASSP)*, April 2015, pp. 509–513.
- [17] N. Chitanont, K. Yatabe, K. Ishikawa, and Y. Oikawa, "Spatio-temporal filter bank for visualizing audible sound field by Schlieren method," *Appl. Acoust.*, vol. 115, pp. 109–120, 2017.
- [18] K. Yatabe, R. Tanigawa, K. Ishikawa, and Y. Oikawa, "Time-directional filtering of wrapped phase for observing transient phenomena with parallel phase-shifting interferometry," *Opt. Express*, vol. 26, no. 11, pp. 13705–13720, May 2018.
- [19] K. He, J. Sun, and X. Tang, "Guided image filtering," *IEEE Trans. Pattern Anal. Mach. Intell.*, vol. 35, no. 6, pp. 1397–1409, June 2013.
- [20] N. Fukushima, K. Sujimoto, and S. Kamata, "Guided image filtering with arbitrary window function," in *2018 IEEE Int. Conf. Acoust. Speech Signal Process. (ICASSP)*, 2018, pp. 1523–1527.
- [21] C. Tomasi and R. Manduchi, "Bilateral filtering for gray and color images," in *6th Int. Conf. Comput. Vis. (IEEE Cat. No.98CH36271)*, Jan 1998, pp. 839–846.
- [22] Y. Oikawa, M. Goto, Y. Ikeda, T. Takizawa, and Y. Yamasaki, "Sound field measurements based on reconstruction from laser projections," in *2005 IEEE Int. Conf. Acoust. Speech Signal Process.*, March 2005, vol. 4, pp. iv/661–iv/664.
- [23] M. J. Hargather, G.S. Settles, and M.J. Madalis, "Schlieren imaging of loud sounds and weak shock waves in air near the limit of visibility," *Shock Waves*, vol. 20, no. 1, pp. 9–17, Feb 2010.
- [24] A. Torras-Rosell, S. Barrera-Figueroa, and F. Jacobsen, "Sound field reconstruction using acousto-optic tomography," *J. Acoust. Soc. Am.*, vol. 131, no. 5, pp. 3786–3793, 2012.
- [25] K. Ishikawa, K. Yatabe, Y. Ikeda, and Y. Oikawa, "Numerical analysis of acousto-optic effect caused by audible sound," in *12th West. Pac. Acoust. Conf. (WESPAC)*, Dec. 2015, pp. 165–169.
- [26] H. Schreiber and J. H. Bruning, *Phase Shifting Interferometry*, chapter 14, pp. 547–666, Wiley-Blackwell, 2006.
- [27] Y. Awatsuji, M. Sasada, and T. Kubota, "Parallel quasi-phase-shifting digital holography," *Appl. Phys. Lett.*, vol. 85, no. 6, pp. 1069–1071, 2004.
- [28] J. E. Millerd, N. J. Brock, J. B. Hayes, M. B. North-Morris, M. Novak, and J. C. Wyant, "Pixelated phase-mask dynamic interferometer," *Proc. SPIE*, vol. 5531, pp. 5531–5531–11, 2004.
- [29] T. Onuma and Y. Otani, "A development of two-dimensional birefringence distribution measurement system with a sampling rate of 1.3 MHz," *Opt. Commun.*, vol. 315, pp. 69–73, 2014.
- [30] X. Su and W. Chen, "Reliability-guided phase unwrapping algorithm: a review," *Opt. Lasers Eng.*, vol. 42, no. 3, pp. 245–261, 2004.
- [31] Q. Kemaoy, W. Gao, and H. Wang, "Windowed Fourier-filtered and quality-guided phase-unwrapping algorithm," *Appl. Opt.*, vol. 47, no. 29, pp. 5420–5428, Oct 2008.
- [32] G. Paál and I. Vaik, "Unsteady phenomena in the edge tone," *Int. J. Heat Fluid Flow*, vol. 28, no. 4, pp. 575–586, 2007.
- [33] M. K. Ibrahim, "Experimental and theoretical investigations of edge tones in high speed jets," *J. Fluid Sci. Technol.*, vol. 8, no. 1, pp. 1–19, 2013.